Optical Coupling of Whispering-Gallery Modes of Two Identical Microdisks and Its Effect on Photonic Molecule Lasing

Elena I. Smotrova, *Student Member, IEEE*, Alexander I. Nosich, *Fellow, IEEE*, Trevor M. Benson, *Senior Member, IEEE*, and Phillip Sewell, *Senior Member, IEEE*

***Abstract*—The lasing characteristics of a photonic molecule in the form of two optically coupled semiconductor microdisks are investigated. Electromagnetic analysis of the lasing spectra and linear thresholds of the coupled whispering-gallery (WG) modes of four different symmetry classes is presented. Here, Maxwell's equations and accurate boundary and radiation conditions are considered as a specific "cold-cavity-with-gain" eigenvalue problem. Each eigenvalue is a pair of real-valued parameters -frequency and threshold material gain. In the two-dimensional (2-D) approximation, based on the introduction of an effective refractive index, this problem is reduced to a determinant equation with favorable features. A secant-type method is further used to calculate thresholds and lasing frequencies numerically. Results obtained show that optical coupling may lead to a further reduction of the ultralow thresholds of the WG modes, although the opposite, i.e., threshold spoiling, is more common.**

***Index Terms*—Laser, microdisk, photonic molecule, whispering-gallery (WG) modes .**

I. Introduction

LASING is a complicated phenomenon involving the joint action of several physical mechanisms, the most important of which are carrier transport, stimulated emission of photons, heating, and optical (i.e., electromagnetic) field confinement. To respond to the challenge of the comprehensive modeling of a semiconductor laser, one needs to take full account of all these effects. However, the complexity of the analysis can be reduced in a well-known manner, by solving the so-called "cold-cavity" problem where optical modes are viewed as solutions to electromagnetic theory equations with appropriate boundary conditions.

Microdisk lasers were first demonstrated in the 1990s as extremely compact sources of light [1]–[11]. Lasing in disks of 1–10 μm diameter and 100–200 nm thickness, containing layers of quantum wells, boxes, and dots, was achieved both with a photopump and the injection of current. Disk materials used were, e.g., GaAs/InGaAsP (emission wavelength around 1550 nm), ZnSe/CdS (510 nm), ZnO/SiO2 (390 nm), and InGaN/GaN (370 nm). The main features of such lasers are 1) several periodically spaced lasing frequencies, 2) ultralow thresholds, and 3) predominantly in-plane light emission. The disk modes were identified as quasi-whispering-gallery (WG) modes confined at the rim due to almost total internal reflection. Note that the three-dimensional (3-D) problem for a thinner-than-wavelength disk can be approximately reduced to the two-dimensional (2-D) problem in the disk plane, with the effective-index approach [12]. The WG modes in the isolated disk have been described using many techniques, ranging from a WKB analytical study to finite-difference time-domain (FDTD)-based numerical approximations [7]–[11].

Previously, cold-cavity modeling of microlasers was done by calculating the natural modes of the passive open dielectric resonators. (The FDTD approach to this needs a remark. The FDTD-based numerical codes that are popular today are not able to solve the eigenvalue problem in a direct manner. They need a pulsed source placed inside a cavity, so that evaluation of the natural frequencies and Q-factors is done via studying the transient response.) Here, one is interested in the complex-valued natural frequencies ω, and the modes with the largest Q-factors (i.e., the smallest values of $\mathrm{Im}\omega$) are associated with lasing. To explain the measured lasing frequencies, one may assume, for example, that the modal electric field vanishes at the disk rim. Rough estimation of Q-factors, on the other hand, needs a much finer technique, taking into account, for example, tunneling considerations. However, it is easy to see that in this way, the lasing phenomenon is not addressed directly—the specific value of threshold gain needed to force a mode to become lasing is not included in the formulation. At the same time, it is known that each eigenfrequency is a function of the gain parameter, say γ. Hence, one can look for a specific value of γ that brings the function $\mathrm{Im}\omega(\gamma)$ to zero and consider this as the threshold of lasing (because then the radiation losses are balanced exactly with macroscopic gain).

Therefore, in [13], we proposed the lasing eigenvalue problem (LEP) specifically tailored to extract not only frequencies, but also threshold gains from the field equations. Refining this analysis, in [14] we accurately accounted for the thin-disk effective index dispersion and demonstrated a good agreement with published experimental data. We have also studied the effect of the gain nonuniformity (e.g., due to the ring electrodes [15]) on the thresholds of the WG modes in a single microdisk.

At the present time, much experimental attention is been paid to the manufacture and study of microcavity laser arrays [16]. The reason for this is a hope to achieve efficient

Manuscript received February 10, 2005. This work was supported in part by EPSRC-UK under Grant GR/S60693/01P, in part by the Royal Society under Grant IJP-2004/R1-FS, and in part by INTAS-EU under Grant 04-83-3340.

E. I. Smotrova and A. I. Nosich are with the Institute of Radio-Physics and Electronics of the National Academy of Sciences of Ukraine (IRE NASU), Kharkiv 61085, Ukraine (e-mail: elena_smotrova@yahoo.com).

T. M. Benson and P. Sewell are with the George Green Institute for Electromagnetics Research, University of Nottingham, Nottingham NG7 2RD, U.K.

Digital Object Identifier 10.1109/JSTQE.2005.862940

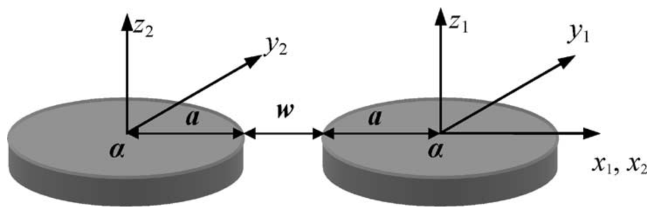

Fig. 1. 3-D geometry of two optically coupled circular disk semiconductor microresonators forming a photonic molecule.

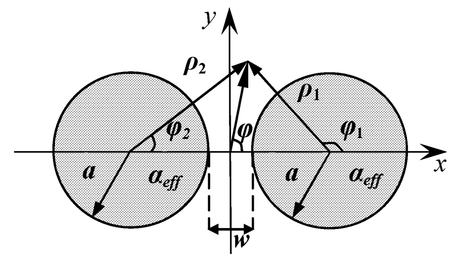

Fig. 2. 2-D geometry of two optically coupled circular resonators.

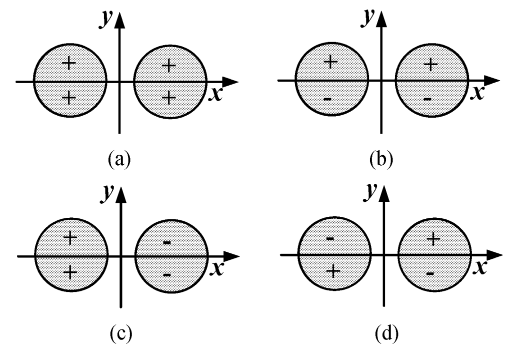

Fig. 3. Four classes of field symmetry. (a) *x-even/y-even (EE)*. (b) *x-odd/y-even* (OE). (c) *x-even/y-odd* (EO). (d) *x-odd/y-odd (OO)*.

power combining, and an overall improvement of emission performance for high-density photonic integrated circuits. Accurate theoretical analysis of lasing in optically coupled microcavities seems to be absent, although a study of coupled WG modes was attempted in [17] with the FDTD method (see[1]). On the other hand, recent experiments with "photonic molecules" formed by two microresonators showed the splitting of the modes into symmetry classes that may have quite different lasing properties [18], [19].

The goal of the present paper is accurate study of the LEP for a pair of optically coupled identical circular microresonators supporting WG modes. In Section II, we formulate the LEP for the 2-D model of a two-disk laser with uniform gain. In Section III, we consider four independent classes of modes in terms of the two-fold symmetry of such a structure. In Section IV, we study spectra and thresholds for the two-disk laser with uniform gain, and show that thresholds can be lowered relatively to the single-disk ones. Corresponding near fields and far-field emission patterns are discussed in Section V. Conclusions are presented in Section VI. In the Appendix, the formulation of the eigenfrequency problem for the complex-valued natural frequencies and generalized natural modes of an open resonator is summarized for comparison with the LEP as a more adequate model of the lasing phenomenon.

II. 2-D Lasing Problem for Two Microdisks

Fig. 1 shows two identical microdisk cavities located in the same plane in free space. Suppose that each disk has thickness d, radius a, and real-valued refractive index α. The separation between the disks is denoted as d. The time dependence $e^{-i\omega t}$ is implied, and the free-space wavenumber is $k = \omega/c = 2\pi/\lambda$, where λ is wavelength.

Assume that we have already reduced the problem to the 2-D model by using the effective-index model [14]. Then we can consider two identical circular resonators with effective refractive index α_{eff} and air gap w—see Fig. 2.

Here, we can treat two polarization states separately, with the aid of one function U, which is either the E_z or the H_z field component. The LEP statement implies (see [14], [15]) that U must satisfy the 2-D Helmholtz (A1) where, if $r < a$, the coefficient α_{eff} is replaced with the complex-valued parameter $\nu = \alpha_{\text{eff}}^{H,E}(q) - i\gamma$; otherwise $\alpha_{\text{eff}} = 1$. Here, the effective index is associated with the qth guided wave of a slab of the same thickness as the disk $(1 < \alpha_{\text{eff}(q)}^{H,E} < \alpha)$ [15]. In this paper, we shall assume that the material gain $\gamma > 0$ is constant, i.e., uniform across the disks. At the disk rims, $L : (\rho_{1,2} = \alpha)U(\rho_2 = a)$, and the transparency conditions (A2) hold, with $\beta^H = \nu^{-2}$ and $\beta^E = 1$. The condition of the local finiteness of energy is given by (A3). Thanks to the real-valued k, U obeys the usual 2-D radiation condition (A4) and does not diverge at infinity.

Considering the LEP, we look for two real numbers, $\kappa = ka$ and γ. The first is the normalized lasing frequency, and the second is the linear threshold material gain. Obviously, the lasing threshold γ, extracted from the LEP, cannot be simply derived from the Imk for the eigenfrequency problem (see Appendix), because ν enters the LEP not only as a product with k, but also independently.

The basic properties of the lasing eigenvalues can be established, even before the computations, for an arbitrary-shaped open resonator. The proof is based on the analytical regularization; i.e., the equivalent reduction of the boundary-value problem to a set of Fredholm second-kind integral or matrix equations [20], and the use of the operator extensions of the Fredholm theorems [21]. It is found that:

1) all $\gamma > 0$, so that thresholdless lasing is not possible;
2) eigenvalues form a discrete set on the plane (k, γ);
3) each eigenvalue has finite multiplicity;
4) no finite accumulation points of eigenvalues exist;
5) each eigenvalue (i.e., each lasing frequency and each threshold) is a piece-continuous function of resonator shape L, separation w, and refractive index α, and this property can be lost only if eigenvalues coalesce;
6) moving on the (k, γ) plane, eigenvalues can disappear only at infinity.

III. Four Classes of Symmetry

The geometry in Fig. 2 has twofold symmetry. Therefore, it is clear from general considerations that all possible field functions split into four different independent classes of symmetry with respect to the x and y-axes.

We introduce three polar coordinate systems: two local systems associated with each resonator, $(\rho_{1,2}, \varphi_{1,2}$, and a global system, (ρ, φ)- see Fig. 2. Taking into account conditions (A1) and (A3), we expand the field function inside each cavity as

$$U_{1,2}(\rho,\varphi) = \sum_{p=(0)1}^{\infty} A_p^{1,2} J_p(k\nu\rho_{1,2}) S_p(\varphi_{1,2}), \quad \rho_{1,2} < a \qquad (1)$$

where J_m is the Bessel function, and $S_p(\varphi_i) = \cos p\varphi$ for the x-even modes and $\sin p\phi$, for the x-odd modes $(i = 1, 2)$.

In the free space, the field function is a superposition of expansions generated by both resonators and satisfying (A4)

$$U(\rho,\varphi) = \sum_{p=0(1)}^{\infty} B_p^1 H_p^{(1)}(k\rho_1) S_p(\varphi_1) + \sum_{p=0(1)}^{\infty} B_p^2 H_p^{(1)}(k\rho_2) S_p(\varphi_2) \qquad (2)$$

where $H_p^{(1)}$ is the Hankel function of first kind.

In order to satisfy the requirements of symmetry or antisymmetry with respect to the j-axis, we impose the following conditions, respectively:

$$U(x,0) = 0 \quad \partial U(x,y)/\partial y|_{y=0} = 0. \qquad (3)$$

The use of addition theorems for cylindrical functions enables us to transform the series into the polar coordinate system associated with each cavity. Then, substitution of (2) into (A2) and (3) and introduction of ~~$x_m = A_m^1 J_m(\kappa)$~~ leads to the following four matrix equations: correct: x_m=A^1_mF_m(k,g)J_m(k)

x-even/y-even (EE) and x-even/y-odd (EO) mode classes

$$x_m \pm \sum_{p=0}^{\infty} \mu_p x_p K_{mp}(\kappa,\gamma) \left[H_{m+p}^{(1)}(\kappa l) + (-1)^p H_{m-p}^{(1)}(\kappa l) \right] = 0 \qquad (4)$$

x-odd/y-even (OE) and x-odd/y-odd (OO) mode classes

$$x_m \pm \sum_{p=1}^{\infty} x_p K_{mp}(\kappa,\gamma) \left[H_{m+p}^{(1)}(\kappa l) - (-1)^p H_{m-p}^{(1)}(kl) \right] = 0 \qquad (5)$$

where

$$\mu_0 = 1/2, \mu_{p>0} = 1$$
$$K_{mp}(\kappa,\gamma) = J_m(\kappa) V_p(\kappa,\gamma) [F_p(\kappa,\gamma) J_p(\kappa)]^{-1}$$
$$F_m(\kappa,\gamma) = J_m(\kappa\nu) H_m^{\prime(1)}(\kappa) - \nu\beta^{E,H} J_m'(\kappa\nu) H_m^{(1)}(\kappa)$$
$$V_m(\kappa,\gamma) = J_m(\kappa\nu) J_m'(\kappa) - \nu\beta^{E,H} J_m'(\kappa\nu) J_m(\kappa) \qquad (6)$$

$l = 2 + w/a$ is the normalized distance between the centers of the resonators, and the prime denotes differentiation with respect to the argument.

In operator notation, (4) and (5) can be written as

$$[I + G^{i,j}(\kappa,\gamma)]X = 0 \qquad (7)$$

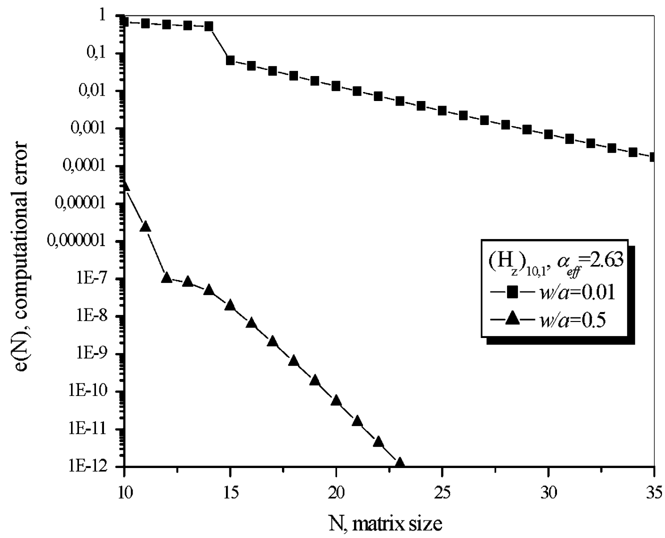

Fig. 4. Error in computation of the EE class versus the matrix truncation number for two values of the separation parameter.

where $X = \{x_p\}_{p=0(1)}^{\infty}, I = \{\delta_{mp}\}_{m,p=0(1)}^{\infty}$ is identity operator, and $G^{i,j} = \{G_{mp}{}^{i,j}\}_{m,p=0(1)}^{\infty}, i,j = \mathrm{E(even), O(odd)}$ are compact operators if $F_p(\kappa,\gamma)J_p(\kappa) \neq 0, p = 0, 1, \ldots$. Therefore, the equations obtained are the Fredholm second kind equations, and their eigenvalues possess the properties listed in Section II. Moreover, as, in fact, $\sum_{m,n=0(1)}^{\infty} |G_{mn}^{i,j}| < \infty$, the search for the LEP eigenvalues is reduced to finding zeros of the determinants of truncated (4) and (5)

$$\mathrm{Det}[I + G^{i,j}(\kappa,\gamma)] = 0 \qquad (8)$$

and convergence to the exact eigenvalues of infinite matrices is guaranteed if the truncation number is increased.

We computed lasing spectra and linear thresholds for coupled semiconductor microdisks with a two-parameter secant-type iterative method [13]. As, in reality, the photoluminescence spectrum has a width of 100 nm or less [1–6, 16–18], it is justifiable to take $\alpha_{\mathrm{eff}} = \mathrm{const}$ when computing a specific optical mode. If, for example, $\lambda_0 = 1.55\ \mu$m and $d = 100$ nm, then $\alpha_{\mathrm{eff}(0)} H = 2.63$. In the same disk, alternatively polarized modes have much smaller effective indices, like $\alpha_{\mathrm{eff}(0)}^E = 1.31$, and can be neglected in view of their very high thresholds [13], [14]. The cylindrical functions in (6) can be calculated to machine precision. As an initial guess, we took the values for κ and γ in a single resonator; i.e., the roots of $F_m(\kappa,\gamma) = 0$.

In Fig. 4, we present the dependences of computational error in determining the eigenvalues $(\kappa,\gamma)_{10,1}$ on the size of the matrix G^{EE}. They demonstrate that to achieve a practical accuracy of 4–5 digits, one needs a few more equations than the normalized optical size of the resonator given by $ka\alpha_{\mathrm{aeff}}$.

IV. Effect of Coupling on Spectra and Thresholds

It is worth remembering that all the lasing modes of an isolated circular cavity split, thanks to the rotational symmetry, into independent families according to the azimuth index m and those with $m > 0$ are twice degenerate [13]. For each family, transparency conditions (A2) generate the characteristic equation $F_m(\kappa, \gamma) = 0$, whose roots (shown in Fig. 3) are the LEP eigenvalues. To number them, a second index n is needed—it corresponds to the number of field variations along the radius. Furthermore, we recall that the effective-index method introduces a third index, q (see [14]), so that, in principle, the roots should be denoted as $(\kappa_{mnq}, \gamma_{mnq}$, where $m, q \geq 0, n \geq 1$. In our numerical study, we shall assume that α_{eff} is associated with the principal (even) slab wave, and omit the corresponding index, $q = 0$.

The lasing spectra and thresholds of a GaAs microdisk of thickness $d = 0.1a$, computed with account of the dispersion of effective indices of two principal slab waves, TE_0 and TM_0, were presented in [14]. They show that the plane (κ, γ) is inhabited by the LEP eigenvalues in a nonuniform manner. One can clearly distinguish between the non-WG modes, which have very high thresholds $\gamma > 0.01$ and $\gamma \approx \text{const}/\kappa$, and the true WG modes. The latter have $m/\alpha_{\text{eff}} < \kappa < m$ and display drastically smaller thresholds, $\gamma \approx \text{const}\, e^{-\kappa}$. These eigenvalues form inclined "layers" on the plane (κ, γ), and the lowest (in terms of γ), layer corresponds to the radial index $n = 1$.

In Figs. 5 and 6, we present the dependences of lasing frequencies and thresholds on the normalized separation parameter w/a for the WG modes of the families $(H_z)_{5,1}$ and $(H_z)_{10,1}$ of all four symmetry classes. They show, firstly, that if the separation gets smaller, then the WG modes obtain frequency shifts—two of the four are redshifted by almost identical amounts, and two others are blueshifted. Secondly, if the separation becomes smaller than a certain critical value, then the thresholds of all four modes get considerably higher than for the isolated disk. However, if the separation is comparable to λ, it is possible to achieve a threshold that is somewhat lower than the limit one for $w \to \infty$.

V. Near Fields and Emission Patterns

In Fig. 7, we present the near fields of the photonic-molecule WG modes of the H_z-type belonging to the quartet of $(H_z)_{5,1}$ modes. They show that the near-fields of the EE and OE mode classes experience a greater degree of perturbation, up to the merging together of the adjacent field spots of separate resonators, than the modes of the other two symmetry classes, EO and OO, whose fields are odd with respect to the y-axis. Note that geometrical optics fails to quantify the coupled mode fields, and FDTD-based analysis (see [18]) generates only transient excitation fields that are quite far from steady-state ones.

Far-field emission patterns (see (A4)) are given by

$$\Phi(\varphi) = \sum_{p=0}^{\infty} \mu_p (-i)^p \left(B_p^1 \pm (-1)^p B_p^2\right) \times (e^{-i\tau} \pm (-1)^p e^{i\tau}) S_p(\varphi) \quad (9)$$

where $\tau = (\kappa l/2) \cos\varphi$, and the coefficients are expressed as

$$B_p^1 = -\pi\kappa x_p V_p(\kappa, \nu)[2iJ_p(\kappa)F_p(\kappa)]^{-1},$$
$$B_p^2 = \pm(-1)^p B_p^1. \quad (10)$$

Here, the sign "+" corresponds to the modes of the EE and OO symmetry classes, and the sign "−" corresponds to the modes of the EO and OE classes.

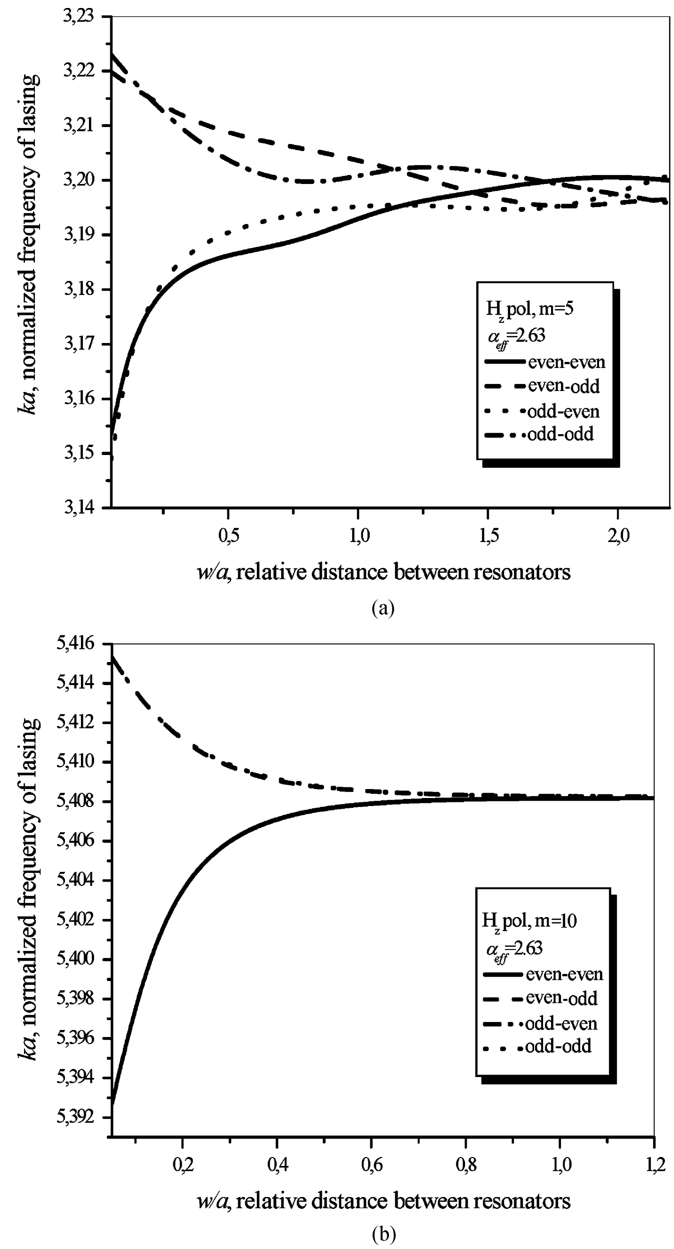

Fig. 5. Normalized lasing frequencies for the modes of the families (a) $(H_z)_{5,1}$ and (b) $(H_z)_{10,1}$, in two coupled GaAs disk resonators, $\lambda = 1.55, \alpha = 3.374$, and $d/a = 0.1$.

To quantify the directionality of light emission, it is convenient to use the value of directivity borrowed from the theory of antennas

$$D = \frac{2\pi}{P} |\Phi(\varphi_{\max})|^2, \quad P = \int_0^{2\pi} |\Phi(\varphi)|^2 \, d\varphi \quad (11)$$

where $\varphi_{\max}$ is the angle of a main beam radiation and P is, within a constant, the total power radiated by a lasing mode.

In Fig. 8, the plots of the directivity and the main beam orientation angle in the first quadrant are given versus the separation parameter w/a, for the coupled $(H_z)_{5,1}$ modes of all four symmetry classes. Note that omnidirectional emission results in

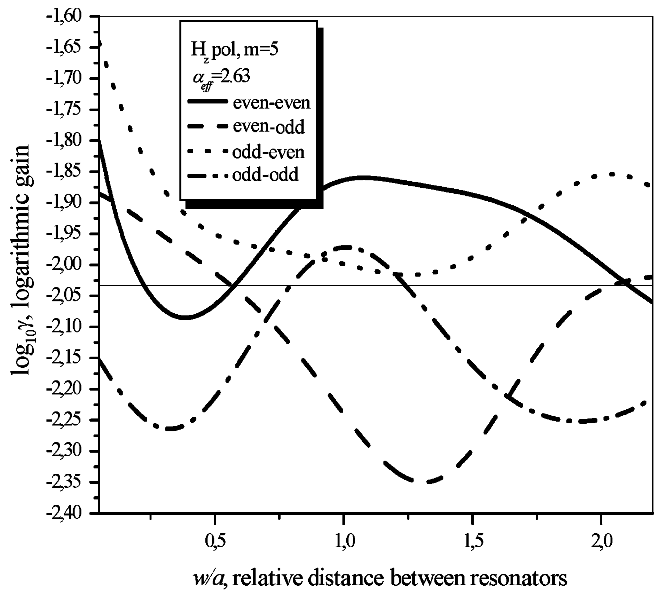

(a)

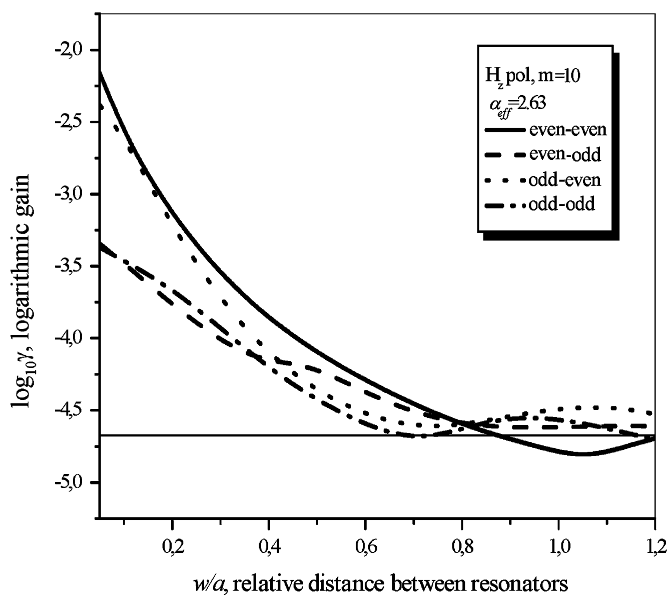

(b)

Fig. 6. Threshold gains of the modes of families (a) $(H_z)_{5,1}$ and (b) $(H_z)_{10,1}$, in two coupled GaAs disk resonators, $\lambda = 1.55$ nm, $\alpha = 3.374$, and $d/a = 0.1$. The straight line is the threshold of the corresponding mode in single microdisk.

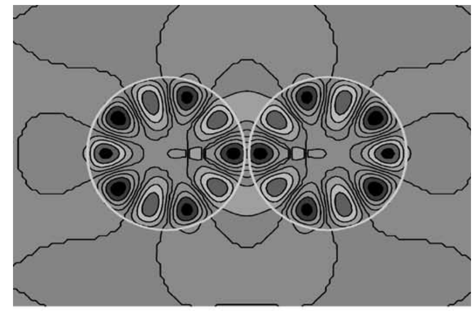

(a)

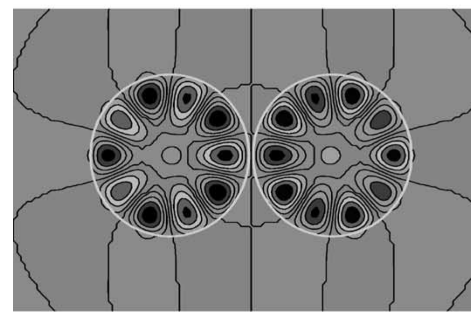

(b)

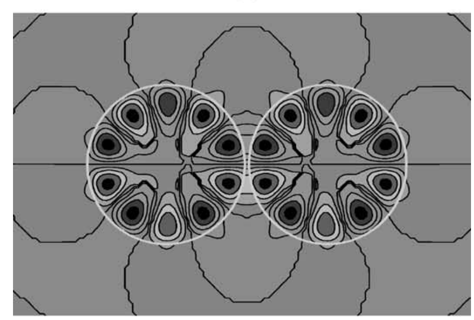

(c)

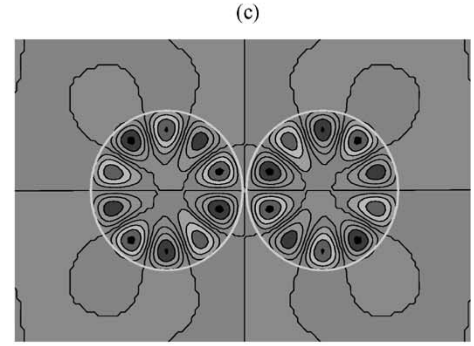

(d)

Fig. 7. Near-field portraits of four $(H_z)_{5,1}$ modes, $\alpha_{\text{eff}} = 2.63, w/a = 0.05$. (a) *x-even/y-even*, $ka = 3.15, \gamma = 1.58 * 10^{-2}$. (b) *x-even/y-odd*, $ka = 3.22, \gamma = 1.3 * l0^{-2}$. (c) *x-odd/y-even*, $ka = 3.15, \gamma = 2.29 * l0^{-2}$. (d) *x-odd/y-odd*, $ka = 3.22, \gamma = 7.03 * 10^{-3}$.

$D = 1$, and that all modes of a single circular resonator (with $\Phi(\varphi) = \cos m\varphi$ or $\sin m\varphi$) have $D = 2$. Thus, the coupling of the lasing cavities enables enhancement of directionality. The main beam orientation angle reveals jumps at certain values of separation. This is because all beams vary both in orientation and in strength, so that different beams play the role of the "main" beam at different separations.

The inserts show the normalized emission patterns of the four WG modes of two resonators with separations corresponding to the maximum directivities (marked with arrows). They show that, normally, there are four identical main beams of emission (due to the two-fold symmetry); however, sometimes they merge into two beams along one of the symmetry axes. At the "jump points" in the main-beam angle dependences, the number of equally strong beams is, correspondingly, eight or four. Note that the OO modes of the "twice-odd" symmetry cannot have less than four main beams, and thus they display generally smaller values of directivity.

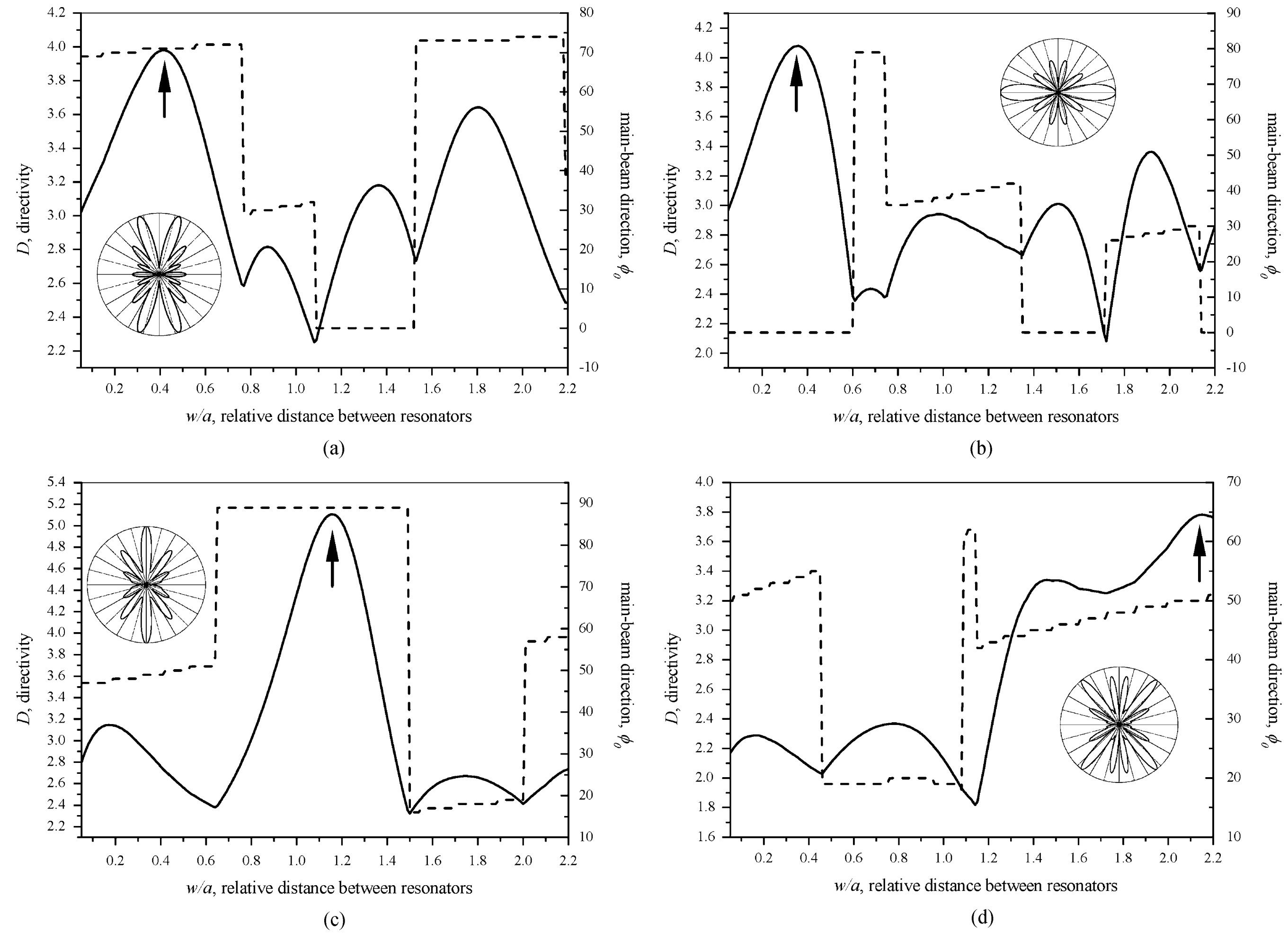

Fig. 8. Dependences of the emission directivity (solid lines) and main-beam radiation angle (dashed lines) on the normalized distance between two resonators, for the $(H_z)_{5,1}$ modes. $\alpha_{\text{eff}} = 2.63$. Mode classes (a) EE, (b) EO, (c) OE, (d) OO. Far-field patterns are shown for the maximum directivities.

VI. Conclusion

We have demonstrated that the "cold-cavity" linear thresholds of two identical, proximity-coupled, semiconductor microdisk lasers forming a photonic molecule can be lowered with respect to the corresponding mode thresholds of a photonic atom; i.e., a single disk. This is found from a specialized eigenvalue problem; i.e., the LEP. However, such a reduction of threshold is relatively small and needs precise tuning of the separation between resonators. Furthermore, instead of two degenerate WG modes of each azimuth-index family in a single circular resonator, the modes of two coupled resonators fall into one of four classes forming the quartets, each mode of the quartet having different symmetry properties across the x and the y-axes. The threshold reduction mentioned may, in principle, take place for the modes of any class of symmetry. However, multimode lasing within a mode quartet may occur if the gain exceeds the level of several thresholds. Bringing the resonators closer to each other than some critical distance boosts the thresholds of modes of all four classes.

The electromagnetic fields of the coupled WG modes of a photonic molecule display more complicated portraits than for a single resonator, and cannot be explained with simple ray-tracing considerations. In the far-field zone, coupled modes have more directive emission patterns than single-cavity modes, and may display two or four identical dominant beams due to the two-fold symmetry of the structure studied.

The LEP is easily adaptable to study arrays of microdisks with nonuniform gain; e.g., if ring electrodes are used for current injection. More complicated cavity shapes can be analyzed by using the boundary IE method described in [22].

Appendix

Complex-Frequency Eigenvalue Problem

The 2-D boundary-value problem for the in-plane modal field $U(r, \varphi)$ involves the Helmholtz equation

$$\left[\frac{1}{r}\frac{\partial}{\partial r}\left(r\frac{\partial}{\partial r}\right) + \frac{1}{r^2}\frac{\partial^2}{\partial \varphi^2} + k^2\alpha_{\text{eff}}^2\right] U(r, \varphi) = 0 \qquad \text{(A1)}$$

where the refractive index is $\alpha_{\text{eff}} = \alpha_{\text{eff}}^{H,E}$ inside the cavity and 1 outside, and transparency conditions on the contour

L are

$$U^-(r,\varphi)|_L = U^+(r,\varphi)|_L,$$
$$\left.\frac{\partial U^-(r,\varphi)}{\partial r}\right|_L = \beta^{H,E}\left.\frac{\partial U^+(r,\varphi)}{\partial r}\right|_L \quad \text{(A2)}$$

where the superscripts "±" indicate the limiting values from inside and outside of L, respectively, $\beta^H = (\alpha^H_{\mathrm{eff}(q)})^{-2}$, and $\beta^E = 1$. The field function must also satisfy the condition of the local energy finiteness

$$\int_D (|kU|^2 + |\mathrm{grad} U|^2) r dr d\varphi < \infty, \qquad D \subset (r,\varphi) \quad \text{(A3)}$$

and a condition at infinity. If k were real-valued, one could impose the Sommerfeld radiation condition [22]

$$U(r,\varphi) \sim (2/i\pi kr)^{1/2} e^{ikr}\Phi(\varphi), \qquad r\to\infty \quad \text{(A4)}$$

However, Poynting's theorem, applied to an eigenfunction $U(r,\varphi)$ leads to the conclusion that, independently of the geometry of the open resonator, real-valued eigenwave-numbers do not exist. To comply with the physical situation, it is necessary to admit complex values of k. In 2-D, the Green's function of (A1) is the outgoing Hankel function $H_0^1(kr)$, whose domain of analytic continuation is the Riemann surface of the function Lnk. Therefore, analytic continuation of the 2-D Sommerfeld condition to all complex k has the form known as the Reichardt condition (see in [23], Appendix)

$$U(r\varphi) \sim \sum_{s=-\infty}^{\infty} a_s H_s^{(1)}(kr) e^{is\varphi}, \qquad r\to\infty \quad \text{(A5)}$$

Thus, (A1)–(A3) and (A5) form a most general frequency eigenvalue problem in 2-D. Then, the same Poynting theorem leads to the conclusion that on the 0-th sheet of Lnk, the eigenwavenumbers can only be located in the lower halfplane. Hence, each of them has a negative imaginary part for the selected time dependence (it would be positive if it were $e^{i\omega t}$). In this sense they are generalized eigenvalues with corresponding generalized eigenfunctions $U(r,\varphi)$ that diverge at infinity as $O(e^{|\mathrm{Im}k|r} r^{-1/2})$.

Note that one cannot simulate a spontaneous emission rate enhancement by studying a dipole radiating from an open cavity with gain. This is because if the dipole frequency coincides with a lasing frequency, the enhancement is unlimited. To overcome this difficulty, one has to introduce time dependence and saturation; i.e., nonlinearity.

Acknowledgment

The authors are grateful to A. Y. Poyedinchuk and S. V. Boriskina for valuable discussions.

References

[1] S. L. McCall, A. F. J. Levi, R. E. Slusher, S. J. Pearson, and R. A. Logan, "Whispering-gallery mode microdisk lasers," *Appl. Phys. Lett.*, vol. 60, no. 3, pp. 289–291, 1992.

[2] R. E. Slusher, A. F. J. Levi, U. Mohideen, S. L. McCall, S. J. Pearson, and R. A. Logan, "Threshold characteristics of semiconductor microdisk lasers," *Appl. Phys. Lett.*, vol. 63, no. 10, pp. 1310–1312, 1993.

[3] T. Baba, M. Fujita, M. Kihara, and R. Watanabe, "Lasing characteristics of GalnAsP-InP strained quantum-well microdisk injection lasers with diameter of 2–10 μm," *IEEE Photon. Technol Lett.*, vol. 9, no. 7, pp. 878–880, Jul. 1997.

[4] B. Corbett, J. Justice, L. Considine, S. Walsh, and W. M. Kelly, "Low-threshold lasing in novel microdisk geometries," *IEEE Photon. Technol. Lett.*, vol. 8, no. 7, pp. 855–857, Jul. 1996.

[5] B. Gayral, J. M. Gererd, A. Lemaitre, C. Dupuis, L. Mamin, and J. L. Pelouard, "High-Q wet-etched GaAs microdisks containing InAs quantum boxes," *Appl. Phys. Lett.*, vol. 75, no. 13, pp. 1908–1910, 1999.

[6] H. Cao, J. Y. Xu, W. H. Xiang, Y. Ma, S. H. Chang, and S. T. Ho, "Optically pumped InAs quantum dot microdisk lasers," *Appl. Phys. Lett.*, vol. 76, no. 24, pp. 3519–3521, 2000.

[7] M. K. Chin, D. Y. Chu, and S. T. Ho, "Estimation of the spontaneous emission factor for microdisk lasers via the approximation of whispering gallery modes," *J. Appl. Phys.*, vol. 75, no. 7, pp. 3302–3307, 1994.

[8] N. C. Frateschi and A. F. J. Levi, "The spectrum of microdisk lasers," *J. Appl. Phys.*, vol. 80, no. 2, pp. 644–653, 1996.

[9] R. P. Wang and M.-M. Dumitrescu, "Optical modes in semiconductor microdisk lasers," *IEEE J. Quantum Electron.*, vol. 34, no. 10, pp. 1933–1937, Oct. 1998.

[10] B.-J. Li and P.-L. Liu, "Numerical analysis of the whispering-gallery modes by the FDTD method," *IEEE J. Quantum Electron.*, vol. 32, no. 9, pp. 1583–1587, Sep. 1996.

[11] M. Fujita, A. Sakai, and T. Baba, "Ultrasmall and ultralow threshold GalnAsP-InP microdisk injection lasers: Design, fabrication, lasing characteristics, and spontaneous emission factor," *IEEE J. Sel. Topics Quantum Electron.*, vol. 5, no. 3, pp. 673–681, May/Jun. 1999.

[12] G. R. Hadley, "Effective index model for VCSELs," *Opt. Lett.*, vol. 20, pp. 1483–1485, 1995.

[13] E. I. Smotrova and A. I. Nosich, "Mathematical analysis of the lasing eigenvalue problem for the WG modes in a 2-D circular dielectric microcavity," *Opt. Quantum Electron.*, vol. 36, no. 1–3, pp. 213–221, 2004.

[14] E. I. Smotrova, A. I. Nosich, T. M. Benson, and P. Sewell, "Cold-cavity thresholds of microdisks with uniform and non-uniform gain: Quasi-3D modeling with accurate 2D analysis," *IEEE J. Sel. Topics Quantum Electron.*, vol. 11, no. 5, pp. 1135–1142, Sep./Oct. 2005.

[15] M. Kneissl, M. Teepe, N. Miyashita, N. M. Johnson, G. D. Chen, and R. K. Chang, "Current-injection spiral-shaped microcavity disk laser diodes with unidirectional emission," *Appl. Phys. Lett.*, vol. 84, no. 14, pp. 2485–2487, 2004.

[16] K. Fetter, T. Kipp, C. Heyn, D. Heitmann, and C. Schuller, "Fabrication of large periodic arrays of AlGaAs microdisks by laser-interference lithography and selective etching," *Appl. Phys. Lett.*, vol. 81, no. 4, pp. 592–594, 2002.

[17] S. Deng and W. Cai, "Discontinuous spectral element method modeling of optical coupling by WG modes between microcylinders," *J. Opt. Soc. Amer. A*, 2004, submitted for publication.

[18] M. Bayer, T. Gutbrod, J. P. Reithmaier, A. Forchel, T. L. Reinecke, P. A. Knipp, A. A. Dremin, and V. D. Kulakovskii, "Optical modes in photonic molecules," *Phys. Rev. Lett.*, vol. 81, no. 12, pp. 2582–2585, 1998.

[19] Y. Kara, T. Mukayama, K. Takeda, and M. Kuwata, "Photonic molecule lasing," *Opt. Lett.*, vol. 28, no. 24, pp. 2437–2439, 2003.

[20] A. I. Nosich, "MAR in the wave-scattering and eigenvalue problems: Foundations and review of solutions," *IEEE Antennas Propag. Mag.*, vol. 41, no. 3, pp. 34–49, 1999.

[21] S. Steinberg, "Meromorphic families of compact operators," *Arch. Rat. Mech. Anal.*, vol. 31, no. 5, pp. 372–379, 1968.

[22] S. V. Boriskina, T. M. Benson, P. Sewell, and A. I. Nosich, "Accurate simulation of 2-D optical microcavities with uniquely solvable boundary integral equations and trigonometric Galerkin discretization," *J. Opt. Soc. Amer. A*, vol. 21, no. 3, pp. 393–402, 2004.

[23] D. Colton and R. Kress, *Integral Equation Method in Scattering Theory*. New York: Wiley, 1983.

[24] S. V. Boriskina, T. M. Benson, P. Sewell, and A. I. Nosich, "Effect of a layered environment on the complex natural frequencies of two-dimensional WGM dielectric ring resonators," *J. Lightw. Technol.*, vol. 20, no. 8, pp. 1563–1572, Aug. 2002.

Elena I. Smotrova (S'03) was born in Kharkiv, Ukraine, in 1980. She received the M.Sc. degree in applied mathematics from the Kharkiv National University, Kharkiv, Ukraine, in 2002. She is currently a Ph.D. student in Radio Physics at the Institute of Radio-Physics and Electronics of the National Academy of Sciences of Ukraine, Kharkiv, Ukraine.

Her research interests are in integral equation methods, eigenvalue problems, and microcavity laser modeling.

Ms. Smotrova received the Young Scientist Prize at the MSMW-04 international symposium.

Alexander I. Nosich (M'94–SM'95–F'04) was born in Kharkiv, Ukraine, in 1953. He received the M.Sc. degree in radio physics and the Ph.D. and D.Sc. degrees from the Kharkiv National University in 1975, 1979, and 1990, respectively.

Since 1978, he has been with the Institute of Radio-Physics and Electronics (IRE) of the National Academy of Sciences of Ukraine, Kharkiv, where he holds a post of Leading Scientist in the Department of Computational Electromagnetics. Since 1992, he has held Research Fellowships and Visiting Professorships in the EU, Turkey, Japan, and Singapore. His interests include methods of analytical regularization, free-space and open-waveguide scattering, complex mode behaviour, radar cross-section analysis, modelling of laser microcavities, and antenna simulation.

Trevor M. Benson (M'95–SM'01) was born in Sheffield, U.K., in 1958. He received the B.Sc. degree in physics (first class honors) and the Ph.D. degree in electronic and electrical engineering from the University of Sheffield in 1979 and 1982, respectively, and the D.Sc. degree from the University of Nottingham in 2005.

After spending over six years as a Lecturer at University College Cardiff, he joined the University of Nottingham Nottingham, U.K., as a Senior Lecturer in Electrical and Electronic Engineering in 1989. He was promoted to the posts of Reader in Photonics in 1994 and Professor of Optoelectronics in 1996. His present research interests include experimental and numerical studies of electromagnetic fields and waves, with particular emphasis on propagation in optical waveguides and lasers, glass-based photonic circuits, and electromagnetic compatibility.

Prof. Benson received the Clark Prize in Experimental Physics from the University of Sheffield in 1979 and has received the Electronics Letters and J. J. Thomson Premiums from the Institution of Electrical Engineers U.K. He is a Fellow of the Institute of Electrical Engineers, U.K., and the Institute of Physics.

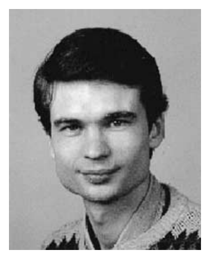

Phillip Sewell (S'88–M'91–SM'04) was born in London, U.K., in 1965. He received the B.Sc. degree in electrical and electronic engineering (first class honors) and the Ph.D. degree from the University of Bath, U.K. in 1988 and 1991, respectively.

From 1991 to 1993, he was an S.E.R.C. Postdoctoral Fellow at the University of Ancona, Italy. Since 1993, he has been with the School of Electrical and Electronic Engineering at the University of Nottingham, Nottingham, U.K., as Lecturer, Reader (since 2001), and Professor of Electromagnetics (since 2004). His research interests involve analytical and numerical modeling of electromagnetic problems, with application to optoelectronics, microwaves, and electrical machines.